

Preliminary communication / Communication

The structural comparison between Al-MCM-41 and B-MCM-41

Mehdi Adjdir^{a,*}, Tewfik Ali-Dahmane^b, Peter G. Weidler^a

^a Institute for Technical Chemistry, Department of Water and Geotechnology (ITC-WGT), Forschungszentrum Karlsruhe GmbH, Hermann-von-Helmholtz-Platz 1, D-76344 Eggenstein-Leopoldshafen, Germany

^b Materials Chemical Laboratory, University of Oran BO: 31100 Oran Es-Sénia, Algeria

Received 19 September 2007; accepted after revision 29 September 2008

Available online 18 November 2008

Abstract

A series of mesoporous aluminosilicate and borosilicate molecular sieves with the MCM-41 structure have been synthesized with different SiO₂/Al₂O₃ or SiO₂/B₂O₃ mass ratios of 5, 10, 25, 50, 70 and 150. The samples were synthesized using the direct method with a duration of 48 h. As silica source colloidal silica (ludox 40%, Prolabo), as aluminium source sodium aluminates and boric acid as the boron source were used in these syntheses. All samples were characterized by X-ray diffraction (XRD), ATR-FT-IR, N₂ gassorption and elemental analysis by electron microscopy.

XRD revealed that the characteristic MCM-41 structure is obtained for both mass ratios greater than 10. B-MCM-41 gives a better organization of the structure than Al-MCM-41. The B substitution in MCM-41 gives a tetrahedral configuration as proven by ATR-FT-IR. The pore diameter is very similar in both samples. *To cite this article: M. Adjdir et al., C. R. Chimie 12 (2009).* © 2008 Académie des sciences. Published by Elsevier Masson SAS. All rights reserved.

Keywords: Al-MCM-41; B-MCM-41; Structure; XRD; ATR-FT-IR; N₂-sorption

1. Introduction

Since the synthesis of the crystalline mesoporous M41S materials by Mobil's researchers [1,2], the following study has focused on the MCM-41 material, which shows a hexagonal array of uniform mesopores with uniform sieves ranging from 2 to 10 nm. Their extraordinary high surface and distinct adsorption properties open up many potential applications in catalysis, separation and nanostructured materials [3–5]. Many researches on MCM-41 have been focused on the incorporation of different elements like aluminium and boron in order to modify the framework of MCM-41 and to

generate catalytic sites needed for different type of reactions. The aluminosilicate mesoporous molecular sieves have received much attention for their strong Brönsted acidity. Many efforts have been made to optimize the silicate sources such as cab-o-sil M5 fumed silica, sodium silicate and tetramethylammonium silicate [6], cab-o-sil M5 fumed silica and sodium silicate [7]. The aluminium source has been studied by Borade and Clearfiled [8], Occeili et al. [9] and Badamali et al. [10] who have reported that the sodium aluminate source incorporates aluminium to a maximum amount in the framework sites. In addition, density and the strength of acid sites are found to be significantly higher when sodium aluminate is applied. The syntheses of Al-MCM-41 by a direct method exhibits considerable hydrothermal stability especially at relatively low Al-contents. The Al-MCM-41 mesoporous

* Corresponding author.

E-mail address: mehdi.adjdir@itc-wgt.fzk.de (M. Adjdir).

materials prepared via grafting routes are extremely stable in boiling water. Regarding the borosilicate mesoporous molecular sieves, Oberhagemann et al. [11] used a single silica source, tetramethoxy silane whereas Trong et al. [12] took Ludox and sodium silicate to synthesize B-MCM-4. It is found [13] that in borosilicate molecular sieves boron occupies the site of the framework aluminium and the protonic form of borosilicate molecular sieves, are less acidic than their aluminosilicate counterparts due to lack of strong Brønsted acidity. In literature no report is available on comparison between B-MCM-41 and Al-MCM-41 with different contents of aluminium and boron. Here we report the synthesis and characterization of MCM-41 materials with different contents of aluminium and boron. We have studied the effect of the $\text{SiO}_2/\text{Al}_2\text{O}_3$ or $\text{SiO}_2/\text{B}_2\text{O}_3$ ratios from 5 to 150 on the final structure and compared their physical properties.

2. Experimental

2.1. Starting materials

Sodium aluminate (54% Al_2O_3 ; 41% Na_2O ; 5% H_2O ; Aldrich) was used as the aluminium sources, boric acid (H_3BO_3 Aldrich) for the provision of boron. Colloidal silica (Ludox 40%, Prolabo) served as a silicon source and as surfactant cetyltrimethylammonium bromide ($\text{C}_{19}\text{H}_{42}\text{NBr}$; CTAB, Aldrich; 99%). Tetramethylammonium hydroxide ($\text{TMAOH}\cdot 5\text{H}_2\text{O}$, 25 wt.%, Aldrich) was utilized as a base.

2.2. Direct synthesis of Si-MCM-41

The synthesis procedure of Si-MCM-41 was reported in a previous paper [14] according to the following molar composition $1\text{SiO}_2:0.25\text{CTAB}:0.2\text{TMAOH}:40\text{H}_2\text{O}$. Tetramethylammonium hydroxide was dissolved in distilled water, and then 2 g of bromide of cetyltrimethylammonium (CTAB) was added into the suspension under stirring. After 30 min, Ludox was slowly added, giving rise to white slurry. The reaction mixture was continuously stirred for 2 h. Afterwards the obtained hydrogel was transferred into a Teflon autoclave vessel for the crystallization, which lasted 48 h at 373 K. Thereafter, the product was washed several times with demineralised water, filtered and dried at 373 K overnight, afterwards calcined under air at 823 K for 12 h.

2.3. Synthesis of B-MCM-41

The hydrothermal synthesis of B-MCM-41 samples was carried out at 373 K using gel with molar

composition of: $1\text{SiO}_2:0.25\text{MCTAB}:0.2\text{TMAOH}:y\text{H}_3\text{BO}_3:40\text{H}_2\text{O}$. The experimental procedure adopted to prepare B-MCM-41 with $y = 5; 10; 25; 50; 70$ and 150 as a typical case is described as follows. A solution was prepared which contains the hydroxide of tetramethylammonium (TMAOH) in demineralised water, then under stirring 2 g of bromide of cetyltrimethylammonium (CTAB) was added. After 30 min silica and finally 0.0193 g of boric acid (H_3BO_3) was added to the solution. The reaction mixture was stirred for 2 h. The hydrogel obtained is heated at 373 K during 48 h. The solid obtained was washed several times with demineralised water, filtered and dried at 373 K overnight, then calcined under air at 823 K for 12 h.

2.4. Synthesis of Al-MCM-41

For this method three solutions were prepared which contain a source of aluminium mixed with an organic hydroxide of quaternary ammonium type (S1), a source of silica (S2) and a surfactant agent (S3). The solvent used in the three solutions is demineralised water. The molar composition was $1\text{SiO}_2:0.25\text{CTAB}:0.2\text{TMAOH}:x\text{Al}_2\text{O}_3:40\text{H}_2\text{O}$, with $x = 5, 10, 25, 50, 70, 150$. The gel was kept in a Teflon-lined stainless steel autoclave and heated at 373 K for two days for crystallization. The solid product obtained was washed, filtered and dried overnight at 373 K. The as-synthesized samples were calcined at 823 K in air for 12 h.

2.5. Characterization

XRD patterns were recorded for all the samples in order to check the formation and structure of Al-MCM-41. The diffraction patterns were recorded in the 2θ range of $1\text{--}12^\circ$ with a step size of 0.02° 2θ and a step time of 5 s on a Bruker D8 diffractometer with $\text{Cu K}\alpha$ ($\lambda = 1.5406 \text{ \AA}$) radiation equipped with PSD counter. A $\text{Cu K}\alpha$ anode was powered with 40 kV and 40 mA. A Talc/Vermiculite mixture was applied as internal standard for peak position correction. Single line fitting was performed with the Bruker software Topas 3.0 (polynom 3rd degree as background, pseudo-voigt function as profile function).

N_2 -sorption measurements were performed at 77 K using a Quantachrome Autosorb1 MP. The samples were degassed at 383 K in vacuum for 24 h before measurements. Specific surface areas were calculated by using the Brunauer–Emmett–Teller (BET) method [15]. Pore size distribution curves were calculated using two methods. One is the NLDFT equilibrium

model with cylindrical pore shape based on the DFT/Monte Carlo method [16] and the other uses the relation $D_p = Cd_{100}(\rho V_{\text{meso}}/1 + \rho V_{\text{meso}})^{1/2}$ described by Ulagappan and Rao [17]

Pore volumes were obtained from the amount of N_2 adsorbed at $p/p_o = 0.7$ corresponding to a pore width of 7.1 nm in order to exclude inter-particle pores formed by the powder.

The ATR-FT-IR (attenuated total reflection Fourier transformed IR) spectra were obtained on a Bruker IFS66 with DTGS detector and global source. The ATR device was a Golden Gate single diamond cell and the powder samples were pressed with a torque of 80 cNm on the diamond. Spectra were fitted with Jandel PeakFit software after background subtraction, a Gauss-function was applied for the description of 9 peaks for B-MCM and 6 peaks for Al-MCM.

3. Results and discussion

In the following chapter we are presenting the XRD and ATR-FT-IR data, which will be discussed in

a structural context. In a final chapter the results of the gas adsorption are shown and reviewed.

3.1. X-ray diffraction

The XRD patterns of Al-MCM-41 and B-MCM-41 samples prepared with different mass ratios, as presented in (Fig. 1a and b), showed typical reflections of hexagonal one-dimensional mesoporous MCM-41 structure [2,18,19]. These XRD patterns were characterized by four peaks denoted as (100), (110), (200) and (210). In the samples with a SiO_2/Al_2O_3 ratio of 5 and 10 and for SiO_2/B_2O_3 with a ratio of 5 these peaks were not well developed, indicating a poor crystallinity for these samples. In contrast, for the samples with SiO_2/Al_2O_3 and SiO_2/B_2O_3 mass ratios of 25–150 the peaks were better resolved.

This was also observed by Kresge et al. [1] and Beck et al. [2]. The best structure for Al-MCM-41 and B-MCM-41 was allotted to each mass ratio of 150 which was in agreement with the results found by Oberhagemann [11], Sayari [20] and Sundaramurthy [21]. Isomorphous substitution has been shown to be an effective method to modify the MCM-41 materials [22].

Substitution of elements into the MCM-41 materials could change the $T=O=T$ angle and $T=O$ length ($T=Si$ or substituted element). Kosslick et al. [23] found that the substitution of Si by tetravalent Ge decreased the $T=O=T$ angle and the $T=O$ bond length. Szostak [24] found that the unit cell volumes in zeolite crystal structure could also change with substitution. The unit cell volume of B-ZSM-5 decreases with increasing B-content compared to (Si)-ZSM-5 because B was smaller than Si [24,25]. Contrary to Szostak, the unit cell of B-MCM-41 increases with increasing B-content. For Al-MCM-41

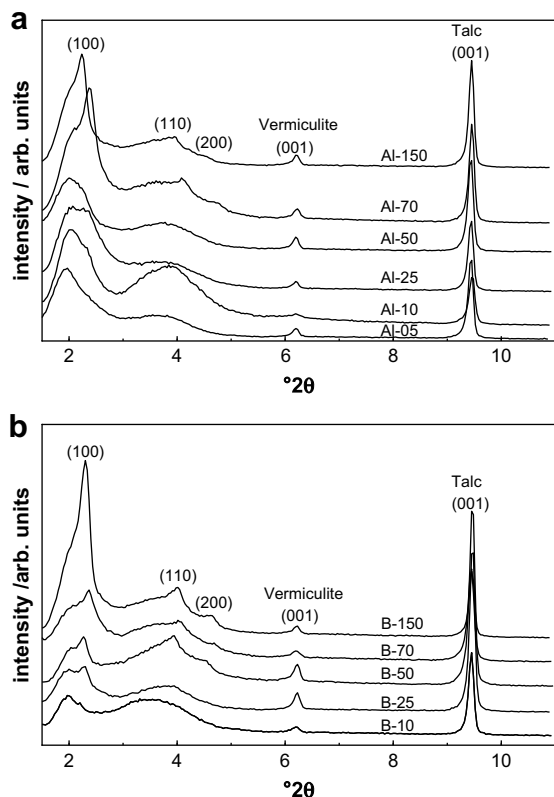


Fig. 1. (a) XRD patterns of Al-MCM-41: Al-5; Al-10; Al-25; Al-50d; Al-70; Al-150. (b) XRD patterns of B-MCM-41: B-5; B-10; B-25; B-50; B-70; B-150.

Table 1
Physical properties of the samples.

Sample	a_0 (nm)	S_{BET} ($m^2 g^{-1}$)	V_{meso} ($cm^3 g^{-1}$)	D_{DFT} (nm)	D_{cal} (nm)	bp (nm)
Si-MCM-41	4.48	1273	0.82	4.0	3.9	0.7
B-MCM-41-150	4.42	1052	0.78	3.8	3.6	0.5
B-MCM-41-70	4.28	576	0.48	3.8	3.2	0.9
B-MCM-41-50	4.50	522	0.47	4.1	3.4	0.6
Al-MCM-41-150	4.52	704	0.58	4.1	3.6	0.6
Al-MCM-41-70	4.27	853	0.67	3.8	3.5	0.7
Al-MCM-41-50	4.91	539	0.48	4.0	3.7	0.7

a_0 : unit cell; S_{BET} : specific surface area; V_{meso} : mesopore volume; D_{DFT} : porous diameter by DFT-Monte carlo method; D_{cal} : porous diameter by the relation $D_{\text{cal}} = Cd_{100}(\rho V_{\text{meso}}/1 + \rho V_{\text{meso}})^{1/2}$; $C = 1.213$ and $\rho = 2.2 \text{ cm}^3/\text{g}$; bp: wall thickness.

Table 2
Results of XRD data evaluation.

Ratio	d_{100} (nm)		a_0 (nm)		FWHM	
	SiO ₂ /B ₂ O ₃	SiO ₂ /Al ₂ O ₃	SiO ₂ /B ₂ O ₃	SiO ₂ /Al ₂ O ₃	SiO ₂ /B ₂ O ₃	SiO ₂ /Al ₂ O ₃
150	3.82	3.91	4.42	4.52	0.199	0.184
70	3.71	3.70	4.28	4.27	0.411	0.318
50	3.90	4.25	4.50	4.91	0.229	0.472
25	3.92	3.76	4.53	4.34	0.464	0.560
10	4.00	3.75	4.62	4.33	0.524	0.516

a weak correlation was found. The unit cell of Al-MCM-41 increases with increasing Al-contents (Table 2 and Fig. 2).

In addition the FWHM of the (100) peak decreased in a progressive way from a mass ratio of 10–150 for both samples (Fig. 3a and b). This could be interpreted in a slight decrease of the ordered nature of MCM-41 through the incorporation of aluminium and boron into the framework. However, in spite of the substitution by these elements the MCM-41 structure was preserved [26,27].

3.2. ATR-FT-IR spectroscopy

The ATR-FT-IR method was particularly suited to record IR spectra of mesoporous materials, such as MCM-41, which were known to exhibit unwanted interaction with KBr [28].

The ATR-FT-IR spectra of Al-MCM-41 (Fig. 4a, Table 3a) exhibited bands in the region between 950 and 1200 cm⁻¹ which could be assigned to antisymmetric stretching of ≡Si–O–T≡ (T = Si or Al) bonds. Bands in the 600–800 cm⁻¹ region will involve the corresponding symmetric vibrations. The

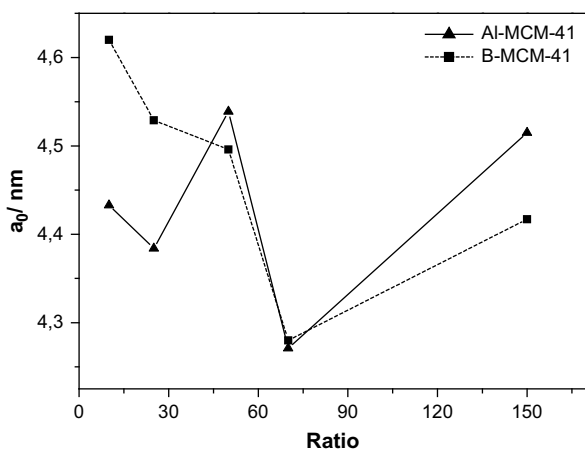


Fig. 2. Relationship between unit cell and ratios.

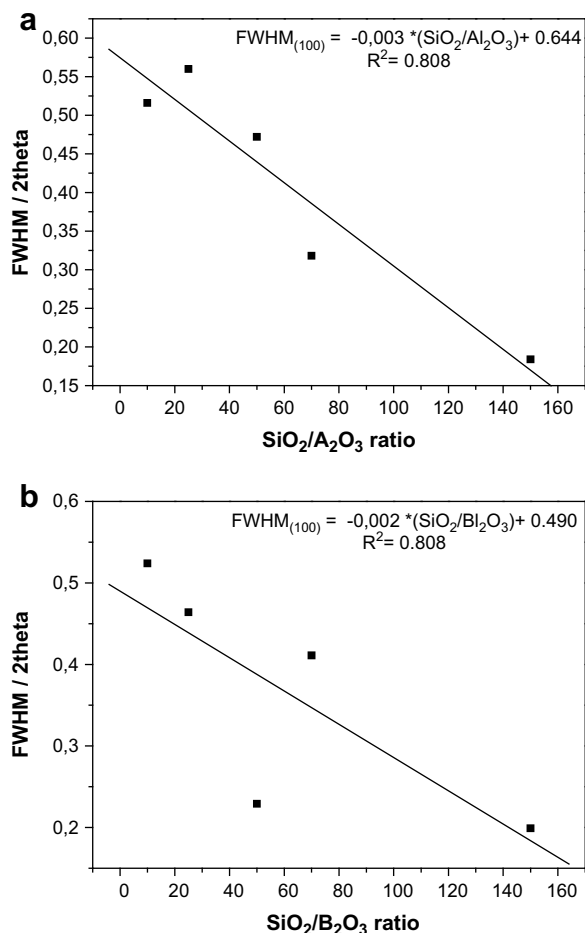


Fig. 3. Linear fit of (a) full width half maximum of SiO₂/Al₂O₃ ratios; (b) full width half maximum of SiO₂/B₂O₃ ratios.

absorption band at 465 cm⁻¹ corresponds to bending vibration of ≡T–O– (T = Si or Al). In addition, there was general tendency for the centre of gravity of the absorption band at 1032–1043 cm⁻¹ to shift to higher frequencies with decreasing aluminium content [29]. All these features are typical of aluminosilicate of MCM-41 structure [26,30].

The vibrations of SiO₂ tetrahedral unit and its modification due to the incorporation of B in the framework mainly appeared in the region of 450–1390 cm⁻¹ (Fig. 4b, Table 3b). The location of boron in samples 25–150 was confirmed from the presence of ATR-FT-IR band at 934–954 cm⁻¹, which was characteristic of tetra-coordinated boron B^[4] in the MCM-41 framework [19,31]. This bond was completely absent in Al-MCM-41. Moreover, a small intensity band at 1395 cm⁻¹ was observed indicating the presence of boron in tri-coordination. A similar observation was reported by Trong et al. [32] and Zhao

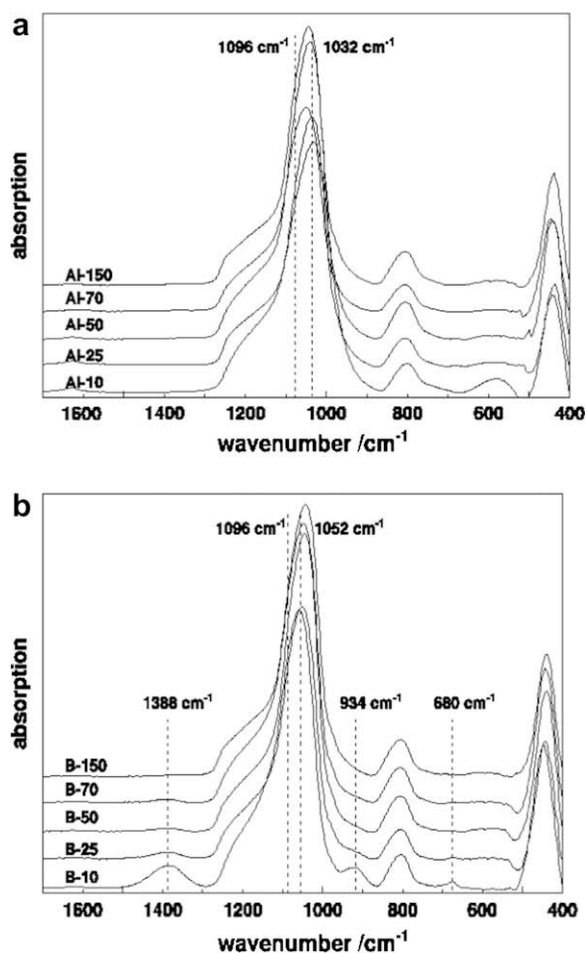


Fig. 4. FT-IR spectra of (a) Al-MCM-41 with various $\text{SiO}_2/\text{Al}_2\text{O}_3$ ratio; (b) B-MCM-41 with various $\text{SiO}_2/\text{B}_2\text{O}_3$ ratios.

et al. [33] in boron incorporated zeolites as well as mesoporous borosilicate materials. However, for the calcined samples (Fig. 4b) a minor band also appeared at $1380\text{--}1396\text{ cm}^{-1}$ which could be assigned to residual tri-coordinated framework boron $\text{B}^{[3]}$. This band formed during the calcinations due to the change of boron coordination from tetrahedral to trigonal [28]. The relative intensity of the 934 cm^{-1} band, characteristic for $\text{B}^{[4]}$ and of the 1390 cm^{-1} band,

characteristic for $\text{B}^{[3]}$ both increase with increasing boron content (Fig. 5). The position of the band at $1043\text{--}1053\text{ cm}^{-1}$ attributed to the Si–O–B bond shifted toward lower wavenumbers with decreasing Boron content.

For the samples with the highest Si content, i.e. a ratio of 150, the positions for the foregoing bands were identical for both Al and B containing samples. By applying a simple spring-model with a force constant K and the reduced mass μ these shifts could be explained. Since the frequency resp. the wavenumber is proportional to $(K/\mu)^{1/2}$, an increase in K and a reduction in μ leads to positive shift in band position. Both apply for Boron. The bond length of Si–B shortens, which would be shown in the following section. Hence the bond strength increased; simultaneously the reduced mass decreased by substituting Si with B. Table 3a and b summarizes the main Al and B-MCM-41 bands.

3.3. Structural discussion

The increasing B-content led to increase $\text{B}^{[3]}$ tri-coordination of boron in the framework (Fig. 5) which moreover led to an increase in unit cell and the particle size of the B-MCM-41 materials. Valerio et al. [34] found that in the case of a proton being the counterion, the tetrahedral BO_4 coordination was unstable and was replaced by silanol groups. These were formed on the adjacent silicon and trigonally coordinated boron. This distance between B and OH (silanols) was longer (0.23 nm) than the corresponding to a tetra-coordinated B (Fig. 6).

The FWHM data from both B- and Al-MCM suggested a less ordered structure for the latter (Table 2 and Fig. 3). The incorporation of boron and aluminium modified the structure from hydrophobic to hydrophilic and gave less well developed structure than Si-MCM-41.

The changes in the unit cell dimensions of MCM-41 material as a function of Si-substitution by Al and B were well documented and were useful to characterize such substitution (Fig. 2).

Table 3a

IR band positions of B-MCM-41 in cm^{-1} .

Si/B ratio	O–Si–O bending	Boron	Si–O–Si sym-stretch	Boron $\text{B}^{[4]}$	Si–O–Si/Si–O–B antisym-stretching				Boron $\text{B}^{[3]}$
10	449.2	679.6	806.5	934.1	1052.6	1096.2	1139.7	1209.7	1388.5
25	445.2	674.7	807.6	959.0	1050.0	1096.8	1144.1	1216.5	1392.2
50	442.5		807.4	956.2	1044.2	1091.9	1136.4	1209.8	1391.8
70	443.3		808.9	954.6	1045.1	1091.2	1135.6	1209.1	1395.4
150	441.9		807.8		1042.7	1089.2	1138.1	1217.5	

$\text{B}^{[4]}$ tetra-coordinations; $\text{B}^{[3]}$ tri-coordinations.

Table 3b
IR band positions of Al-MCM-41 in cm^{-1} .

Si/Al ratio	O–Si–O bending	Si–O–Si sym-stretch	Si–O–Si/Si–O–Al antisym-stretching			
5	443.0	801.2	1031.9	1093.6	1153.1	1214.4
10	439.1	807.1	1037.5	1087.3	1141.9	1218.4
25	442.5	806.5	1040.0	1090.7	1146.9	1217.3
50	445.5	808.3	1048.1	1093.0	1143.1	1216.4
70	441.2	807.9	1044.8	1090.7	1144.6	1219.4
150	441.9	807.8	1042.8	1090.5	1142.3	1215.9

Quantum-chemical calculations suggested that the bond between boron and the protonated framework oxygen atom (silanol group) was much weaker than the Al–O bond in a corresponding $\text{Al}\cdots\text{O}(\text{H})\text{--Si}$ group. The B–O bond in $\text{B}\cdots\text{O}(\text{H})\text{--Si}$ groups was effectively broken, resulting in trigonal boron in the zeolite framework, $\text{B}^{[3]}$. Stave and Nicholas [35] have calculated the B–O and Al–O distances in $(\text{X})_3\text{Si--OH--T}(\text{X})_3$ ($\text{X} = \text{OSiH}_3$, $\text{T} = \text{B}$, Al) cluster models of zeolites ZSM-5 using density functional theory. These authors found a B–O distance of 208.4 pm which is too large for a covalent interaction, while the Al–O bond has a distance of 183.6 pm [35].

3.4. Nitrogen adsorption studies

Substitution of elements into the MCM-41 materials could change the surface properties and the pore structure due to change in the T=O=T angle and T=O length ($\text{T} = \text{Si}$ or substituted element). Kosslick et al. [23] found that the substitution of Si by tetra-valent Ge decreased the T=O=T angle and the T=O bond length.

The influence of this change was also observed in the N_2 gas adsorption for the samples Al-MCM-41 and

B-MCM-41 ($\text{SiO}_2/\text{Al}_2\text{O}_3$ or $\text{B}_2\text{O}_3 = 50, 70$ and 150) synthesized at 373 K (Fig. 7a and b). The isotherms exhibited a type IV isotherms according to the classification of the IUPAC [15]. The results obtained were in agreement with the study carried out by Kosslick et al. [23] and Sayari et al. [20], which allotted lower specific surface area of the Boron containing samples. During the calcination process, trigonal B was lost. It could be assumed that this loss has in influence either in the particle size and/or the porosity, indicated by a decrease of SSA of over $500 \text{ m}^2/\text{g}$ when compared to the Si-MCM-41 (Table 1). The mesopore volume decreased from $0.82 \text{ cm}^3/\text{g}$ for the unsubstituted samples to $0.47 \text{ cm}^3/\text{g}$ for the B and to $0.48 \text{ cm}^3/\text{g}$ for the Al-containing samples.

This could be explained for B-MCM by an expulsion of trigonal boron which leads to a loss of channels. Boron has shown a strong tendency to be leached out of the lattice during calcinations [13]. This further confirmed the mesoporous nature of the samples [36,37].

The pore sizes distributions of all samples were narrow and exhibited a maximum in the range of 3–4 nm (Fig. 8a and b). When compared to siliceous

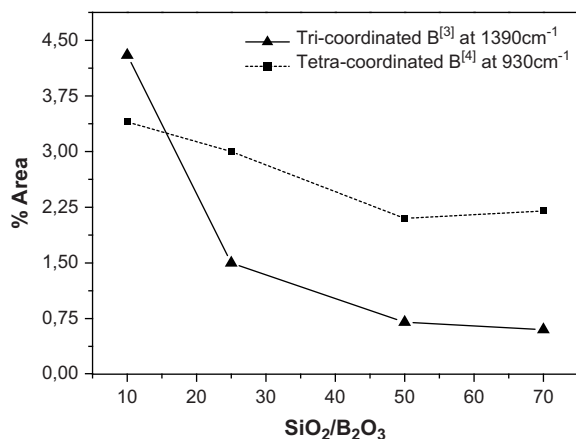


Fig. 5. Tetra- and tri-coordinated boron versus $\text{SiO}_2/\text{B}_2\text{O}_3$ ratios.

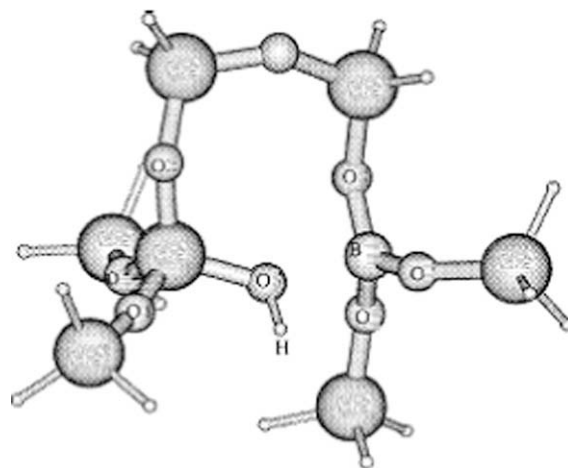


Fig. 6. Optimized model structures with proton as boron counterions [25].

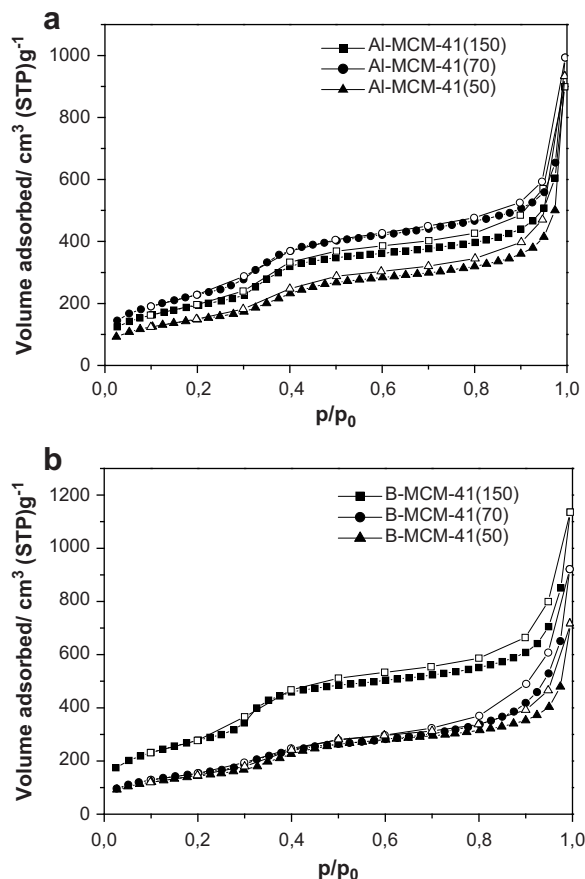


Fig. 7. (a) and (b) Sorption of nitrogen at 77 k for (a) different SiO₂/Al₂O₃ ratios 50, 70 and 150; (b) different SiO₂/B₂O₃ ratios 50, 70 and 150.

MCM-41, the average pore diameter values of B-MCM-41 samples were slightly less and for Al-MCM-41 about the same (Table 1).

The comparison of pore size data derived from DFT theory and from the calculation method from Ulagappan and Rao [17] was in good agreement. The pore wall thickness obtained from the XRD data and the gas adsorption values were 0.7 nm for both substitutions, where B-MCM-41 exhibited a slight larger standard deviation. The value of 0.7 nm resembled the one found for Si-MCM-41 [1,2]. These values can be only considered as estimations, because there is not yet a definitive method for such pore size or pore wall calculation, respectively, because all are implying a smooth cylindrical pore shape. The existence of such a model is a matter of ongoing scientific dispute.

All the textural characteristics of B-MCM-41 and Al-MCM-41 samples revealed that aluminium and boron incorporation slightly decreased the ordered

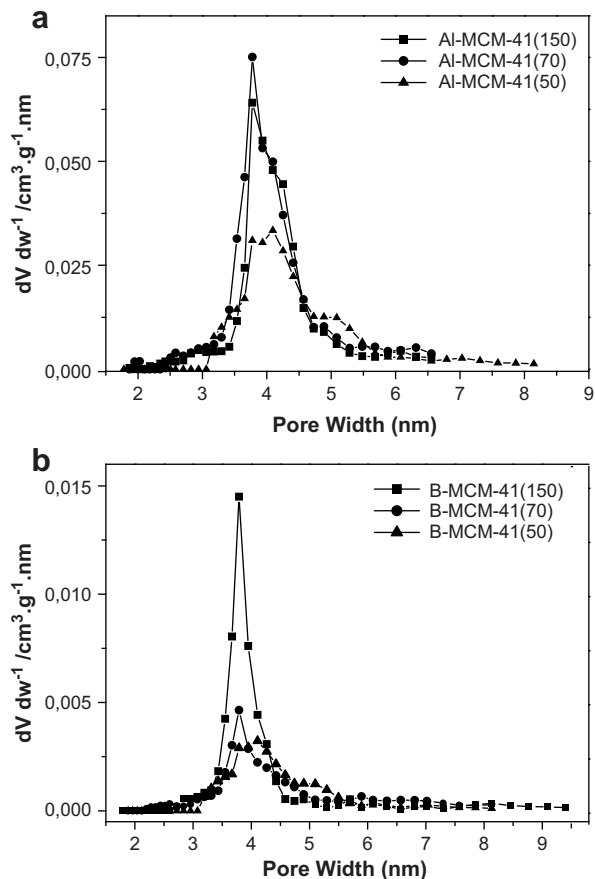


Fig. 8. (a) and (b) Pore distributions of (a) Al-MCM-41 with different SiO₂/Al₂O₃ ratios 50, 70 and 150; (b) B-MCM-41 with different SiO₂/B₂O₃ ratios 50, 70 and 150.

nature of the hexagonal structure of MCM-41. Similar observation was made in XRD analysis (Fig. 2)

4. Conclusion

Isomorphous substitution of boron and aluminium in MCM-41 framework was successfully carried out by a direct synthesis method. The change in d-spacing and unit cell parameter compared to siliceous MCM-41 indicated the incorporation of boron or aluminium in the framework. The nitrogen adsorption studies showed that the synthesized M-MCM-41 materials led to a mesoporous material with narrow pore size distribution. The presence of bands at 1380, 920 and 960 cm⁻¹ in the ATR-FT-IR spectra of all samples confirmed that B was incorporated into the MCM-41 framework. In addition, the shift of the Si–O–M (M = Al, B) band at around 1043 cm⁻¹ gave another strong argument for the incorporation of Al and B.

The best structure was allocated to Al- and B-MCM-41 for a mass ratio equal to 150.

A hexagonal structure characteristic for a mesoporous material produced by the direct synthesis method was still obtained for a $\text{SiO}_2/\text{Al}_2\text{O}_3$ or B_2O_3 ratio of 10. A higher content of Al or B did not further increase the quality of the product.

Acknowledgments

The authors are grateful to The Mr Hans Hunsinger Thermal Waste Treatment Division Institute for Technical Chemistry, Forschungszentrum Karlsruhe for his technical assistance. This work was supported by the DAAD Deutscher Akademischer Austausch Dienst Germany.

References

- [1] C.T. Kresge, M.E. Leonowicz, W.J. Roth, J.C. Vartulie, J.S. Beck, *Nature* 359 (1992) 710.
- [2] J.S. Beck, J.C. Vartuli, W.J. Roth, M.E. Leonowicz, C.T. Kresge, K.D. Schmitt, C.T.-W. Chu, D.H. Olson, E.W. Sheppard, S.B. McCullen, J.B. Higgins, J.L. Schelinker, *J. Am. Chem. Soc.* 114 (1992) 10834.
- [3] M. Vallet-Regi, A. Ramila, R.P. del Real, J. Perez-Pariente, *Chem. Mater.* 13 (2001) 308.
- [4] Z.T. Zhang, Y. Han, W. Zhu, Y. Wang, R.W. Yu, S.L. Qiu, D.Y. Zhao, F.S. Xiao, *Angew. Chem., Int. Ed.* 40 (2001) 1258.
- [5] A. Corma, Q. Kan, M.T. Navarro, J. Perez-Pariente, F. Rey, *Chem. Mater.* 9 (1997) 2123.
- [6] S. Liu, H. He, Z. Luan, J. Klinowski, *J. Chem. Soc., Faraday Trans.* 92 (1996) 2011.
- [7] T. Yanagisawa, T. Shimizu, K. Kudora, C. Kato, *Bull. Chem. Soc. Jpn.* 63 (1990) 988.
- [8] R.B. Borade, A. Clearfield, *Catal. Lett.* 31 (1995) 267.
- [9] M.L. Occelli, S. Biz, A. Auroux, G.J. Ray, *Microporous Mesoporous Mater.* 26 (1998) 195.
- [10] S.K. Badamali, A. Sakthivel, P. Selvam, *Catal. Today* 63 (2000) 291.
- [11] U. Oberhagemann, M. Jeschke, H. Papp, *Microporous Mesoporous Mater.* 27 (1999) 207.
- [12] D. Trong On, P.N. Joshi, G. Lemay, S. Kaliaguine, in: L. Bonnevot, S. Kaliaguine (Eds.), *Zeolites: A Refined Tool for Designing Catalytic Sites*, Elsevier, Amsterdam, 1995, p. 543.
- [13] C.T.-W. Chu, G.H. Kuehl, R.M. Lago, C.D. Change, *J. Catal.* 93 (1985) 45.
- [14] R. Mokaya, *Microporous Mesoporous Mater.* 44–45 (2001) 119.
- [15] IUPAC, *Pure Appl. Chem.* 87 (1957) 603.
- [16] S. Lowell, J.E. Shields, M.A. Thomas, M. Thommes, *Characterization of Porous Solids and Powders: Surface Area, Pore Size and Density*, Springer Verlag, 2006, 347pp.
- [17] N. Ulagappan, C.N.R. Rao, *Chem. Commun.* (1996) 2759.
- [18] P. Selvam, S.K. Bhatia, C.G. Sonwane, *Ind. Eng. Chem. Res* 40 (2001) 3237.
- [19] A.U.B. Queiroz, L.T. Aikawa, French Patent 2694000, 1994.
- [20] A. Sayari, I. Moudrakovski, C. Danumah, C.I. Ratcliffe, J.A. Ripmeester, K.F. Preston, *J. Phys. Chem.* 99 (1995) 16373.
- [21] V. Sundaramurthy, N. Lingappan, *Microporous Mesoporous Mater.* 65 (2003) 243.
- [22] K.F.M.G.J. Scholle, A.P.M. Kentgens, W.S. Veeman, P. Frenken, G.P.M. Van der Velden, *J. Phys. Chem.* 88 (1984) 5.
- [23] H. Kosslick, V.A. Tuan, R. Fricke, Ch. Peuker, W. Pilz, W. Storek, *J. Phys. Chem.* 97 (1993) 5678.
- [24] R. Szostak, *Molecular Sieves*, van Nostrand Reinhold, New York, 1989.
- [25] J. Sauer, in: C.R.A. Catlow (Ed.), *Modelling of Structure and Reactivity in Zeolites*, Academic Press, London, 1992.
- [26] C.Y. Chen, X. H-Li, M.E. Davis, *Microporous Mater.* 2 (1993) 17.
- [27] K. Vidya, S.E. Dapurkar, P. Selvam, S.K. Badamali, N.M. D.KumarGupta, *J. Mol. Catal. A* 181 (2002) 91.
- [28] N. Bai, Y. Chi, Y. Zou, W. Pang, *Mater. Lett.* 54 (2002) 37.
- [29] R.G. Milkey, *Am. Mineral.* 45 (1960) 990.
- [30] B.L. Meyers, S.R. Ely, N.A. Kutz, J.A. Kaduk, E. Van den Bossche, *J. Catal.* 91 (1985) 352.
- [31] I. Eswaramoorthi, A.K. Dalai, *Microporous Mesoporous Mater.* 93 (2006) 1.
- [32] D. Trong On, M.P. Kapoor, L. Bonnevot, S. Kaliaguine, Z. Gabelica, *J. Chem. Soc., Faraday Trans* 1 92 (1996) 1031.
- [33] D. Zhao, Q. Huo, J. Feng, B.F. Chmelka, G.D. Stucky, *J. Am. Chem. Soc.* 120 (1998) 6024.
- [34] G. Valerio, J. Plevert, A. Goursot, F. di Renzo, *Phys. Chem. Chem. Phys.* 2 (2000) 1091.
- [35] M.S. Stave, J.B. Nicholas, *J. Phys. Chem.* 99 (1995) 15046.
- [36] P.J. Branton, P.G. Hall, K.S.W. Sing, *J. Chem. Soc., Chem. Commun.* (1993) 1257.
- [37] D. Franke, G. Schulz-Ekloff, J. Rathousky, *J. Chem. Soc., Chem. Commun.* (1993) 724.